Cross-Country Robotized Vehicles Control: Fuel Saving Technique

V. Kh. Pshikhopov, D. B. Pogosov

***Abstract*—**This paper is about original fuel saving technique and nonlinear multilinked control for tracked robots, equipped with AC electric transmissions. Adequate mathematical model of the cross-country tracked robot, its AC electric transmission and diesel engine are presented. The position-trajectory control method with constant power of the engine together with induction motor optimization technique are introduced. These solutions able to control non-hyperbolic traction drives. Together with fuel saving we provide selectable traction motor optimization. The robot drives with the engine optimal mode and no braking in allowable range of speeds.

***Keywords*—**AC electric transmission, robot control, fuel save, tracked robot.

I. Introduction

TRACKED robots (TR) are advanced systems for transportation, rescue or other tasks. Their development objectives are increasing motion speed, accuracy and optimizing of power consumption.

Usually the unit power ratio of tracked vehicles is low, so the energy optimization problem is important. Extent of energy efficiency in systems equipped with a diesel engine (DE) is fuel consumption rate.

Constant speed of robot motion requires changing torques on the driven sprockets, causing changes DE power in time. From DE theory [1] known that a high dynamics of DE causes higher fuel consumption.

This leads a task of the organization of a robot movement with a constant output power of DE. Control system in this mode should adapt controls to road conditions by changing the chassis speed.

Another problem is a tracked robot maneuvers by its traction drives. This leads the problem of the double coordination of the speed and power: maintain the total power, which taken from DE at constant level and maintain such velocity ratio, as precision trajectory motion.

To reach described advantages, we assume the robot contains an electric transmission, which enables to precision motion on smooth trajectory with, generally, different speeds on driven sprockets. There should be noted, that on traditional (like hydraulic displacement) transmissions such motion modes requires using of brakes. This is not only difficult to accurate control, also a negative effect on the energy efficiency.

This paper introduces a nonlinear control system of tracked robots motion, based on the position-trajectory control method [2]-[3]. Novelty is possibility of movement at mainly constant power, which an engine produced, or with limited of maximum engine power. Non-hyperbolic drives might be used, so no limits for the traction drive mechanical characteristic presents. The electric transmission (ET) we assume based on induction motor drives (ID) and synchronous generator (SG).

This work was supported by the President Grant NSh-3437-2014-10.

Prof. V. Kh. Pshikhopov, is with the Southern Federal University, Rostov-on-Don, 347928, Russia (phone: +7-863-371694; fax: +7-863-371694; e-mail: toe@tgn.sfedu.ru).

D. B. Pogosov, is with the Southern Federal University, Rostov-on-Don, 347928, Russia (phone: +7-863-371694; fax: +7-863-371694; e-mail: deonisiy2004@yandex.ru).

II. Mathematical Model of Control Object

A. Chassis Model of Tracked Robot

We will consider TR with two traction drives (induction motors) and two power (frequency) converters (PC), the traction alternator and the diesel engine. The traction alternator connected to DE through a primary gear. Each traction motor connected to same side driven sprocket through a secondary gear.

Mathematical model of TR introduced by the following system of vector-matrix equations [2], [4]-[7]:

$$\dot{Y} = \begin{bmatrix} P & \varphi \end{bmatrix}^T = R(\varphi) L X \,, \tag{1}$$

$$M\dot{X} = \tilde{Q} - L_2^{-1} F_R \,, \; F_R = F_s f' + L_1^{-1} F_O + F_N \,, \tag{2}$$

$$R(.) = \begin{bmatrix} \cos(.) & \sin(.) \\ -\sin(.) & \cos(.) \end{bmatrix}, \tag{3}$$

$$F_s = \operatorname{diag}((G/2)\cos\alpha\cos\beta)\,,$$

$$F_O = \begin{bmatrix} G\sin\alpha + R_{TR} + F_a & M_r \end{bmatrix}^T ,$$

$$M_r = (\mu G l \cos\alpha\cos\beta(1-(l\xi/2)^2))/4\,,$$

where Y – is vector of the chassis position P and orientation (yaw) φ; $R(.)$ – is a rotation matrix; L, L_1, L_2 – are matrixes of coordinates transformation; X – is vector of the driven sprockets speeds; $\tilde{Q}$ – is vector of the driven sprockets torques; F_R – is vector of a motion resistance; f' – is vector of ground coefficients; M – is matrix of mass and inertia parameters with secondary gears ratio and efficiency; α and β – are pitch and roll, accordingly; G – is weight; l – is length of a track; R_{TR} – is a trailer resistance; F_a – is the air resistance; M_r – is a turn resistance; μ – is coefficient of the turn resistance; ξ – is turn poles shifting; F_N – is vector of immeasurable disturbances, *diag()* – is the function returns its arguments on leading diagonal of a matrix.

B. Electric Transmission Model

An advanced ET based on AC units. In this paper we consider ID with squirrel-cage rotor and SG with salient-pole rotor.

High quality control of AC units is possible by the vector control methods, based on FOC [8]-[10]. According to FOC, voltage and current vectors are calculated in the two-dimensional reference frame $d\ q$, oriented to the rotor flux. Immediate control methods are linear [11-13], intellectual [14] and non-linear [3,8,15].

Basic mathematical model is well known as the Park-Gorev equations. There should be noted, this model does not contain steel losses equations. In paper [8] introduced a good model with additional equations for the rotor flux. In paper [16] introduced series steel losses model.

We introduce the model of ID with different phase numbers [17] by the following equations [8]-[11], [16]:

$$U_d = \sigma L_s \dot{I}_d - \sigma L_s \omega_\Phi I_q + R_1 I_d + L_r^{-1} R_{ms}\Phi + L_r^{-1} L_m \dot{\Phi}, \tag{4}$$

$$U_q = \sigma L_s \dot{I}_q + \sigma L_s \omega_\Phi I_d + R_1 I_q + L_r^{-1} L_m \omega_\Phi \Phi, \tag{5}$$

$$R_1 = R_s + L_r^{-1} L_{\sigma r} R_{ms}, \tag{6}$$

$$R_2 = R_r + R_{mr}, \tag{7}$$

$$R_2^{-1} L_r \dot{\Phi} = (L_m - R_2^{-1} R_{mr} L_r) I_d - \Phi, \tag{8}$$

$$Q = 0.5 Z_m Z_p L_m L_r^{-1} I_q \Phi - k_f \omega, \tag{9}$$

$$R_{mr} = s R_{ms} = s R_m^{-1} \omega_\Phi^2 (s^2+1) L_m^2, \tag{10}$$

$$\omega_\Phi - Z_p \omega = \frac{\left(R_{mr}(L_r + L_m) + L_m R_r\right) I_q}{L_r \Phi}, \tag{11}$$

where U_d, U_q – is the stator voltage vector components; $L_s, L_r = L_m + L_{\sigma r}$ – are the stator and rotor inductances, respectively; L_m – is the main inductance; σ – is the dissipation coefficient; R_s, R_r – are the stator and rotor resistances; R_{ms}, R_{mr} – are the stator and rotor equivalent steel resistances; R_m – is the steel constant resistance; Φ – is rotor flux; I_d, I_q – is the stator current vector components; ω – is the rotor angular velocity; ω_Φ – is the flux angular velocity; Z_p – is quantity of the pair of poles; Z_m – is quantity of the phases; Q – is the torque; k_f – is the friction coefficient, $s = \omega_\Phi^{-1}(\omega_\Phi - \omega)$ – is the slip.

The current is measured and the angle of the rotor flux is calculated according to the method of direct field oriented control [8].

To get the natural phases voltage of AC induction motors, we execute the coordinate transformation (5) by (3):

$$U_{phase} = P_S R^{-1}(\gamma_\omega) U_A,$$

$$P_S = \begin{bmatrix} \sqrt{\dfrac{2}{Z_m}} \cos(j-1)\dfrac{2\pi}{Z_m} & \ldots \\ \sqrt{\dfrac{2}{Z_m}} \sin(j-1)\dfrac{2\pi}{Z_m} & \ldots \end{bmatrix}^T, \ j = \overline{1, Z_m}^T, \dim(P_S) = 2 \times Zm,$$

where U_{phase} – is the natural phases voltage.

We introduce the model of synchronous generator (SD) with different phase numbers [17] by the following equations [8]-[11] :

$$U_{gd} = L_{gd} \hat{\dot{I}}_{gd} + L_{gm} \dot{I}_f + R_g I_{gd} + \omega_g L_{gq} I_{gq}, \tag{12}$$

$$U_{gq} = L_{gq} \hat{\dot{I}}_{gq} - \omega_g L_{gd} I_{gd} + R_g I_{gq} - \omega_g L_{gm} I_f, \tag{13}$$

$$U_f = R_f I_f + L_f \dot{I}_f + L_{gm} \hat{\dot{I}}_{gd}, \tag{14}$$

$$Q_{load} = J_g \dot{\omega}_g = 0.5 Z_{gm} Z_{gp} I_{gq} (L_{gm} I_f + L_\Delta I_{gd}) + k_{fg} \omega_g, \tag{15}$$

$$\omega_g = k_{PG} \omega_e, \tag{16}$$

where U_{gd}, U_{gq} – are the vector components of alternator voltage; R_g – is resistance of the stator winding; ω_g – is SG rotor speed; ω_e – is the DE crankshaft speed; R_f – is resistance of the excitation winding; L_{gd} – is d axes inductance; L_{gq} – is q axes inductance; L_{gm} – is mutual inductance; L_f – is excitation inductance; I_{gd}, I_{gq} – is the stator current vector components; k_{fg} – is the friction coefficient; $L_\Delta = L_{gd} - L_{gq}$; Z_{gp} – is quantity of the pair of poles; Z_{gm} – is quantity of the phases; Q_{load} – is load on alternator shaft; J_g – is inertia of the SG shaft, k_{PG} – the primary gear ratio; U_f – is the excitation voltage; I_f – is the excitation current.

Equation (16) shown connecting DE crankshaft with alternator shaft through the reducer.

Because hardware implementation of power converters is varies [8]-[9], we represent the common case. PC is a two-stage voltage converter: self-excited inverter with DC link. The required voltage vector is implemented by the method of vector PWM conversion, [8], so voltage equation of PC becomes as follows:

$$U_{\max} = \frac{\sqrt{3}}{2} U_{dc},$$

where $U_{\max}$ – is the maximal voltage on ID; U_{dc} – is the voltage on DC link.

C. *Diesel Engine Model*

This paper we assume the diesel combustion engine (DE). The engine characterization [15] shown on Fig.1.

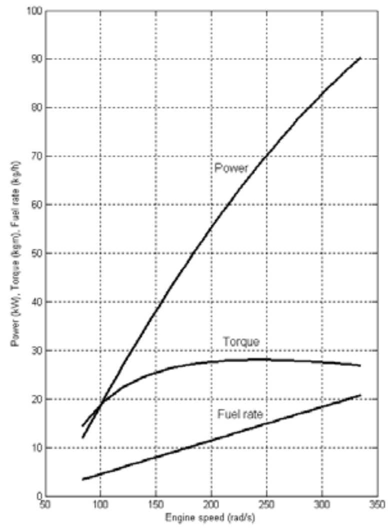

Fig. 1 the diesel engine characteristics: power (kW), torque (kg·m) and fuel rate (kg/h), all depending on engine speed (rad/s)

The curves are shown only for engine speed limited by 330 rad/s, because between 330 rad/s and 420 rad/s the engine torque is drop and power is not raised, so this mode is not useful for constant power motion. At the engine speed more than 420 rad/s the torque is much drop and this mode should be limited in any diesel combustion engine.

The torque model is becomes as follows [1]:

$$J_e \dot{\omega}_e = M_{ind} - M_{fr} - M_{pump}, \tag{17}$$

where J_e – is the engine inertia, M_{ind} – is the indicated engine torque, M_{fr} – is the friction engine torque, M_{pump} – is the pump torque.

Engine torque components can be represented as follows [18]-[19]:

$$M_{ind} = \frac{k_F U_F Q_{LHV} R_{gas} T_{im} (e_0 + e_1 \omega_e + e_2 \omega_e^2)}{\eta_V V_d P_{im}},$$
$$\eta_V = e_3 + e_4 \omega_e + e_5 \omega_e^2,$$
$$M_{fr} = \frac{1000 V_d \left(e_6 + e_7 \omega_e + e_8 \omega_e^2\right)}{2\pi n_R},$$
$$M_{pump} = e_9 P_{im} + e_{10},$$

where U_F – is the fuel rate; Q_{LHV} – is the fuel lower heating value; R_{gas} – is the gas constant, P_{im}; T_{im} – are the pressure and temperature in the intake manifold, respectively; V_d – is the engine volume; η_V – is a volumetric efficiency; n_R – is the number of revolutions for each power stroke, per cycle; $k_F, e_0 - e_{10}$ – are constants. We assume measurable of the intake manifold pressure and temperature.

III. Power Losses and Optimization

A. *Induction Motor Losses and Optimisation*

For the purpose of ET energy consumption optimization, we consider the energy loss in the ID, PC and SG and allocate optimizable losses. In addition, the dependence of the ET efficiency versus useful power is essentially nonlinear. This leads consideration all losses of the energy conversion to DE control. Taking into account the losses allows us controlling ET units with a non-hyperbolic mechanical characteristic. Strictly speaking, the hyperbolic characteristic is ideal and almost unwieldy case.

Mathematical model of IM with squirrel-cage rotor is represented by (5)-(11). Thus, with respect to (4), (5) and (9) the orthogonal components of the current vector represent ID as a two dimensional object. As follows from (9), *q* component of stator current allows to control ID torque and *d* component (8) allows to flux rotor control, i.e. electromagnetic state of ID.

For motion control systems is necessary to guarantee a smooth transition from a system with maximum performance properties to a system with maximum energy efficiency properties, predominantly in the intermediate area of operation. This we can achieve by separating the control channels of ID torque and the rotor flux, with a possibility of separate desired transient on each channel. One matter note is there, this separating is a formal approach, no decomposition. For example, in applications where the quick-action is more important than energy efficiency, increasing the transient time of the rotor flux changing, will allow the control system to fast torque control. Tuning the rotor flux to optimal value at long duration thereby will be without energy losses of force of this process. That is, without deterioration of performance characteristics by capture energy from *q* component of stator current during the torque transient. This mode we named selectable optimisation.

This necessitates the optimization of some function, which is energy loss cost function of IM, depending on the rotor flux and independent of currents, etc. The function may be obtained from the equation of power balance equation, by subtracting therefrom the net power (mechanical work), as well as non-optimizable power losses [20]-[21]:

$$P_{loss,IM} = \frac{Z_m}{2}\left(\frac{dW}{dt} + P_{cur} + P_{flx}\right) + k_f \omega, \tag{18}$$

$$\Lambda = W + P_{cur} + P_{flx}, \tag{19}$$

$$P_{cur} = R_{cur} I_s^2, \tag{20}$$

$$P_{flx} = R_{flx} \Phi^2, \tag{21}$$

$$W = \frac{\sigma L_s I_s^2}{2} + \frac{\Phi^2}{2L_r}, \tag{22}$$

$$R_{cur} = R_1 + \frac{L_m^2}{L_r^2} R_2 - R_{mr}, \tag{23}$$

$$R_{flx} = R_{ms}\left(\frac{L_m}{L_r} - \frac{R_{mr}}{R_2}\right) + \frac{2L_m R_{mr}}{L_r} + \frac{R_2}{L_r^2}, \tag{24}$$

$$I_s^2 = \frac{\Phi^2}{L_m^2} + \frac{4L_r^2 Q^2}{Z_m^2 Z_p^2 L_m^2 \Phi^2}, \tag{25}$$

where $P_{loss,IM}$ – is total IM losses, P_{cur}, P_{flx} – is copper and steel losses of the rotor and the stator, $k_f \omega$ – is friction and windage losses, W – is the stored energy in the magnetic system of IM, I_s – is the stator current (Euclidean norm), Λ – is the cost function.

The magnetic energy is the first integral of the magnetic power. Minimizing this energy is needed to reduce reactive currents.

Using equation (25) we able to represent the function (19) as a function of the rotor flux. We compute the partial derivative of the function (19) of the rotor flux and given follows equations:

$$\frac{\partial \Lambda}{\partial \Phi} = \frac{\partial W}{\partial \Phi} + \frac{\partial P_{cur}}{\partial \Phi} + \frac{\partial P_{flx}}{\partial \Phi} = 0,$$

$$\frac{\partial I_s^2}{\partial \Phi} = \frac{2\Phi}{L_m^2} - \frac{8L_r^2 Q^2}{Z_m^2 Z_p^2 L_m^2 \Phi^3},$$

$$\frac{\partial W}{\partial \Phi} = \frac{\sigma L_s}{2}\frac{\partial I_s^2}{\partial \Phi} + \frac{\Phi}{L_r},$$

$$I_s^2 = \frac{\Phi^2}{L_m^2} + \frac{4L_r^2 Q^2}{Z_m^2 Z_p^2 L_m^2 \Phi^2},$$

$$\frac{\partial P_{cur}}{\partial \Phi} = R_{cur}\frac{\partial I_s^2}{\partial \Phi},$$

$$\frac{\partial P_{flx}}{\partial \Phi} = 2R_{flx}\Phi,$$

The solution is:

$$\Phi_{opt} = \sqrt{Q L_\Phi}, \tag{26}$$

$$L_\Phi = \frac{2L_r}{Z_m Z_p L_m}\sqrt{\frac{\sigma L_s + 2R_{cur}}{0.5\sigma L_s + R_{cur} + L_r^{-1} + 2R_{flx}}},$$

where Φ_{opt} – is the optimal flux, L_Φ – is the irrational function.

B. Traction Alternator and Power Converters Losses

The components of SG voltage and current in the reference frame are depends on its Euclidean norms and angle between the voltage vector and *d* axle. The Euclidean norms are fully determined from necessary ID voltage and currents (4), (5) and (11). The angle between *d* and voltage vector is depend on power factor and skew angle φ_W, namely:

$$\varphi_W = \frac{I_d U_d + I_q U_q}{\|I\|\|U\|} - \arctan(\omega_\Phi C_{dc}),$$

where C_{dc} – is the voltage on the DC link.

Hence, SG is fully determined object, and there is no redundancy, which might have optimised.

We represent total losses of SG and PC by follows equations:

$$P_{loss,SG} = \frac{Z_{gm}}{2}\left(I_g^T L_g \hat{\dot{I}}_g + I_g^T R_g I_g\right) + k_{fg}\omega_g, \tag{27}$$

$$L_g = diag(L_{gd}, L_{gq}),$$

$$P_{loss,f} = R_f I_f^2 + L_f \dot{I}_f I_f, \tag{28}$$

$$P_{loss,inv} = I^2(R_{sc} + P_{sw} f_{PWM}), \tag{29}$$

where $P_{loss,SG}$ – is SG losses, $P_{loss,f}$ – is the excitation losses, $P_{loss,inv}$ – is PC losses, I^2 – is current through PC, R_{sc} – is semiconductor switch resistance, P_{sw} – is elementary switching resistance correspond to losses (depends on switching time), f_{PWM} – is PWM base frequency. At the current angles divisible by 60 degrees, the right summand in (29) is equal to zero.

C. Total Electric Transmission Losses

Total ED losses will be presented as static (time-independent) and dynamic (time-dependent).

Static loss obtained from (16), (18), (20)-(24) and (27)-(28):

$$P_{loss,static} = P_{LSI} + P_{LSF} + K_f X + k_{fg} k_{PG}\omega_e + R_f I_f^2, \tag{30}$$

$$P_{LSI} = I_{s,1}^T \tilde{R}_1 I_{s,1} + I_{s,2}^T \tilde{R}_2 I_{s,2},$$

$$P_{LSF} = \frac{Z_m}{2}\left(R_{flx,1}\Phi_1^2 + R_{flx,2}\Phi_2^2\right),$$

$$P_{loss,f} = R_f I_f^2 + L_f \dot{I}_f I_f,$$

$$P_{loss,f} = R_f I_f^2 + L_f \dot{I}_f I_f,$$

$$K_f = k_f[1 \quad 1],$$

$$\tilde{R}_k = \frac{Z_m}{2} R_{cur,k} + \frac{Z_{gm}}{2} R_g + R_{sc} + P_{sw} f_{PWM,k}, k = \overline{1,2},$$

Dynamic loss obtained from (18), (20)-(24) and (27)-(28):

$$P_{loss,dynamic} = P_{LDI} + \frac{Z_m}{2}\left(\frac{\Phi_1\dot{\Phi}_1}{L_{r,1}} + \frac{\Phi_2\dot{\Phi}_2}{L_{r,2}}\right) + L_f I_f \dot{I}_f, \tag{31}$$

$$P_{LDI} = I_{s,1}^T \tilde{L}_1 \dot{I}_{s,1} + I_{s,2}^T \tilde{L}_2 \dot{I}_{s,2},$$

$$\tilde{L}_k = \frac{Z_{gm}}{2} L_g + \frac{Z_m}{2} diag(\sigma L_{s,k}), k = \overline{1,2}.$$

IV. Synthesis of Control System

Existing control methods for tracked robots are based on the well-developed theory of optimal control [22]. Unfortunately, this theory requires linearization of motion mathematical models and the actual problem is the choice of cost function [22]. On the other hand, applying nonlinear methods, such as the position-trajectory control [3,15] eliminates the above disadvantages.

We define the control system goals as movement on a trajectory at a desired constant power of DE.

We set a TR trajectory by following vector equation [2], as function N_1 of external coordinates (1) in implicit form [23]:

$$\Psi_T = \begin{bmatrix} N_1(P) & 0_3 \end{bmatrix}^T . \tag{32}$$

We set power consumption at desired level wj at steady state, by the following vector equation, as a function of internal coordinates and their derivatives (2):

$$\tilde{W} = \begin{bmatrix} 0 & -\left|X\right|^T M\dot{X} + \left|X\right|^T F_R + P_{loss,static} - wj & 0_2 \end{bmatrix}^T, \tag{33}$$

We set each rotor fluxes at optimal level (26) by follows equations:

$$\tilde{\Phi} = \begin{bmatrix} 0_2 & \Phi_1^2 - \Phi_{opt,1}^2 & \Phi_2^2 - \Phi_{opt,2}^2 \end{bmatrix}^T, \tag{34}$$

We define the desired character of TR motion as a closed-loop system by follows system of vector-matrix equations:

$$\Psi = \Psi_T + A\dot{\Psi}_T , \tag{35}$$
$$\tilde{\Psi} = \Psi + T\tilde{W} + T\dot{\Psi} , \tag{36}$$
$$\tilde{\tilde{\Psi}} = \tilde{\Psi} + C\dot{\tilde{\Psi}} , \tag{37}$$

where A, T and C – are diagonal matrixes of constant coefficients, which define the desired character of the system action and transient.

According to the well-known Lenz principle of the constancy interlinkages, the resulting magnetic flux cannot change abruptly. Therefore, the rotor flux changes slow, so $\ddot{\Phi} \cong 0$. We make follows assumption for calculate torque (9) derivative $\dot{\Phi} \cong (L_m - R_2^{-1} R_{mr} L_r)\dot{I}_d$.

According to the position-trajectory control method [3], we differentiate equations (17) three times, (1) twice and (2), (8), (9) and (33)-(34) once. Then we solve them together with (35)-(37). Then we solve the result with (12)-(16) and at last with (17). Then we differentiate (30) and put into the result equation (31).

So, we obtain the following control algorithm of TR:

$$U_F = K_{ICE}(M_{fr} + M_{pump} + J_e\dot{\omega}_e), \tag{38}$$
$$K_{ICE} = \frac{\eta_V V_d P_{im}}{k_F Q_{LHV} R_{gas} T_{im}(e_0 + e_1\omega_e + e_2\omega_e^2)},$$
$$\dot{\omega}_e = \frac{3Z_g}{2J_g} I_g^T (K_{G1}K_f + K_{G2}I_g),$$
$$K_{G1} = \begin{bmatrix} 0 & 0 \\ 0 & L_{gm} \end{bmatrix}, K_{G2} = \begin{bmatrix} L_\Delta & 0 \\ 0 & 0 \end{bmatrix},$$
$$K_f = K_{G3}^{-1}\left(U_g - L_g\hat{\dot{I}}_g - (R_G + \omega_e L_g D) I_z^T I_z \overline{R}(\hat{\theta}_g + \varphi_W)\right),$$
$$\mathrm{U_g} = \frac{2}{\sqrt{3}}\max(U_1, U_2)^2 \overline{R}(\hat{\theta}_g),$$
$$U_f = \begin{bmatrix} L_f & R_f \end{bmatrix} K_f + \begin{bmatrix} L_{gm} & 0 \end{bmatrix}\hat{\dot{I}}_g , \tag{39}$$
$$U_k = \sigma_k L_{s,k}\dot{I}_k + \left(\omega_{\Phi,k}\sigma_k L_{s,k} D + R_{IM,k}\right) I_k + K_{IM,k}\Phi_k , \tag{40}$$
$$R_{IM,k} = diag\left(R_{1,k} + \frac{L_{m,k}R_{2,k}}{L_{r,k}^2}(L_{m,k} - \frac{R_{mr,k}L_{r,k}}{R_{2,k}}), R_{1,k}\right),$$
$$K_{IM,k} = \begin{bmatrix} L_{r,k}^{-1}(R_{ms,k} - L_{m,k}) & L_{r,k}^{-1}L_{m,k}\omega_{\Phi,k} \end{bmatrix}^T,$$
$$\dot{I}_z = K_0^{-1}\left(K_1 X + K_5 I_z - K_6 F_r - K_7\dot{F}_r + K_z\right),$$
$$K_z = CT(K_W + K_\Phi) + \Psi_T + T(\tilde{W} + \tilde{\Phi}),$$
$$K_{00} = CT(AJRL + AJ_W)M^{-1},$$
$$K_0 = -(K_{00} + CTJ_\Phi)K_m + CTJ_{PI},$$
$$K_1 = CTAJ\ddot{R}L + K_3\dot{R}L + K_4 RL,$$
$$K_2 = K_3 RL + 2CTAJ\dot{R}L - \left|\dot{X}\right|^T M + CTK_f,$$
$$K_3 = (TA + CA + CT)J + 2CTA\Gamma,$$
$$K_4 = (A + T + C)J + (TA + CA + TC)\Gamma + CTA\dot{\Gamma},$$
$$K_5 = K_2 M^{-1} K_m,$$
$$K_6 = K_2 M^{-1} + CT\left|\dot{X}\right|,$$
$$K_7 = K_{00} + CT\left|X\right|^T,$$
$$K_W = [0 \quad Z_m K_{W1} + (2R_f + L_f) I_f\hat{\dot{I}}_f + k_{fg}k_{PG}\hat{\dot{\omega}}_e \quad 0_2]^T,$$
$$K_{W1} = \Phi_1\dot{\Phi}_1(R_{flx,1} + L_{r,1}^{-1}) + \Phi_2\dot{\Phi}_2(R_{flx,2} + L_{r,2}^{-1}),$$
$$K_\Phi = [0_2 \quad 2\Phi_1\dot{\Phi}_1 \quad 2\Phi_2\dot{\Phi}_2]^T,$$
$$J_\Phi = [0_{22} \quad -diag(L_{\Phi,1}, L_{\Phi,2})]^T,$$
$$J_{PI} = \begin{bmatrix} 0_2 & 2\tilde{R}_1 + \tilde{L}_1 & 0_{22} \\ 0_2 & 2\tilde{R}_2 + \tilde{L}_2 & 0_{22} \end{bmatrix}^T,$$
$$\Phi_k\dot{\Phi}_k = R_{2,k}L_{r,k}^{-1}(L_{m,k} - R_{2,k}^{-1}R_{mr,k}L_{r,k}) - \Phi_k^2,$$
$$J_W = \begin{bmatrix} 0_2 & -\left|X\right|^T M & 0_{22} \end{bmatrix}^T, J = \frac{\partial\Psi_T}{\partial Y^T}, \Gamma = \frac{dJ}{dt},$$
$$I_z = \begin{bmatrix} I_1 & I_2 \end{bmatrix}^T,$$
$$k = \overline{1,2},$$

where U_F – is DE fuel rate output, U_f – is SG excitation voltage output, $U_k, k = \overline{1,2}$ – are ID stator voltages output (input for the power converters), others are functional coefficients.

V. SIMULATION

Simulation of the introduced control algorithms (38)-(40) was accomplished in the software package MATLAB.

Chassis TR is presented by (1)-(2) and has the following parameters: weight 12 tons , length 5.5 m, width 3.8 m, inertia is 1150 kg·m^2, radius of the driven wheel is 0.2 m, secondary gear ratio is 1:2. Traction drives are represented by (6)-(7) and have the following parameters: maximum voltage is 400 V, maximum power is 90 kW, $L_s = L_r = 0.2755$, $R_s = 0.1$, $Z_p = 1$. ID works on the linear area of its magnetization characteristic, so all inductances are constant. We neglected the core losses and friction losses. This case the nonlinear function in (26) is a constant $L_\Phi = 0.4076$.

The first test is constant power running on a circle. The task of TR motion (32) is the circle of radius 100 m centered at the origin and the expression (33), corresponding to the stabilization of constant power at level 70 kW. Adjustment matrices (35)-(37) are unitary matrixes. The initial position of the robot is $Y = [90 \quad 0 \quad \pi/4]^T$ and the robot does not move. Simulation time is 287.4 s. Without loss of generality, we represent the motion resistance vector by constants, equal to 4725. After 70 s from the start of simulation, the vector of resistance will increase to 13300 during 20 s. After 170 s from the start of simulation, the vector resistance reduced to 4725 during 20 s. This simple test allows facilitating analysis of the reaction of the system to changing the motion resistance and corresponds to the rise on hill and downhill.

The control system (35)-(37), should provide a stable movement on the trajectory with a root-mean-square error less than 0.3, at steady state.

The result of simulated trajectory presented on Fig.2.

The result of simulated speed and rising resistance of motion presented on Fig.3.

The voltage and current of traction motors, before coordinates transform, presented on Fig.4.

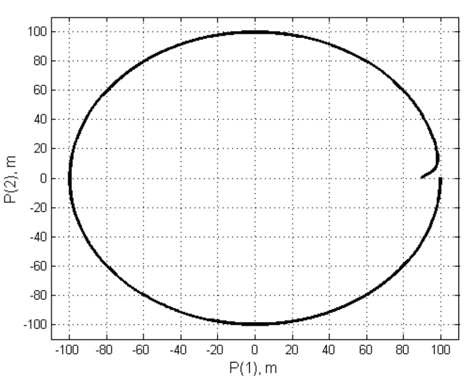

Fig. 2 the trajectory of TR motion, the first test

The root-mean-square error is 0.12 at steady state, which correspond to the requirements. The fuel consumption for this test is 1.1779 kg. The average slip is 2.539% and shown well efficiency of traction drives.

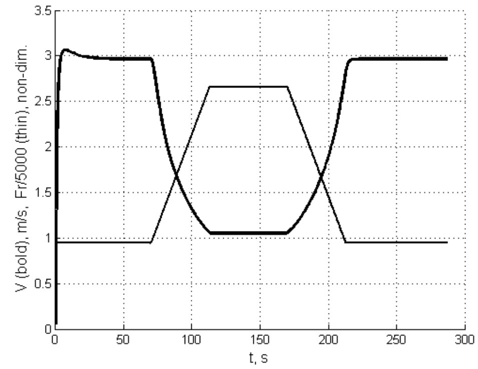

Fig. 3 the speed and motion resistance, the first test (constant power)

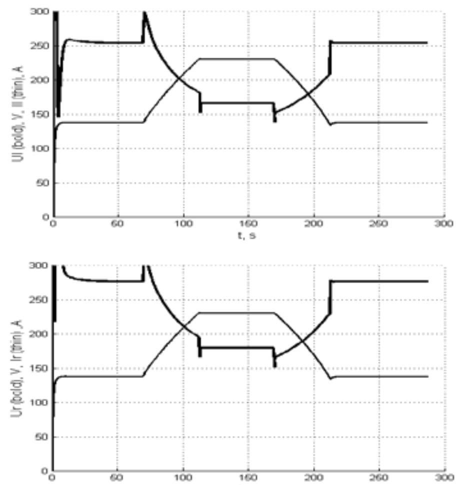

Fig. 4 the traction motors voltage and current, the first test (constant power)

The second test is constant speed running on a circle. The task of TR motion is same, the TR parameters and traction motors parameters are same like the first test. The motion resistance is same too. Constant speed level is 2.2 m/s. This test need to compare fuel consumption of the introduced this paper algorithm and constant speed algorithm from [2]-[3]. Simulation time is 287.4 s.

The result of simulated trajectory is same as in Fig.2, simulated speed and rising resistance of motion presented on Fig.5.

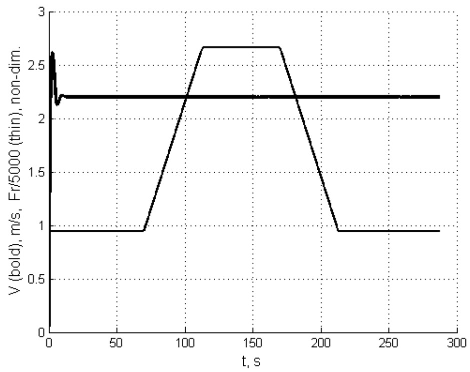

Fig. 5 the speed and motion resistance, the second test (constant speed)

The voltage and current of traction motors, before coordinates transform (9), presented on Fig.6.

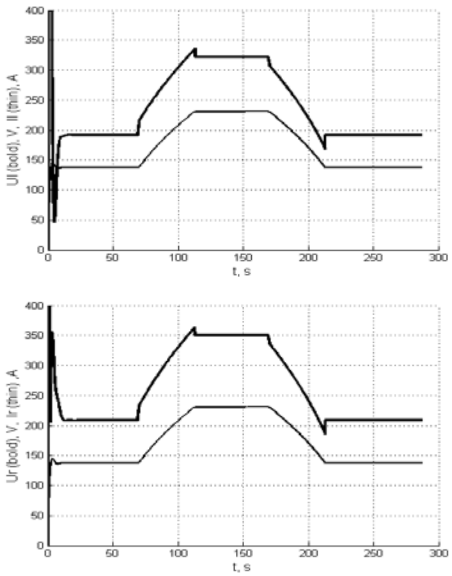

Fig. 6 the traction motors voltage and current, the second test (constant speed)

The fuel consumption for this test is 1.4259 kg. The average slip is 2.342% and shown well efficiency of traction drives.

Therefore, the fuel consumption during the constant power test is 82.6% of the fuel consumption during the constant speed test. Such significant difference is consequence of significant change of the motion resistance (more than three times), which leads to rapid engine acceleration. This is the reason of the high fuel consumption rate in this case. There should be noted that the effectiveness of the introduced algorithm depends on changing the motion resistance during movement. If the changes are minor (in a case of roads), a constant speed might be more preferable for the tasks the organization of transportation or movement in a stream of other objects, moving evenly. However, the proposed algorithms able to significantly reduce fuel consumption for off-road vehicles, such as TR.

VI. Conclusion

Introduced in this paper solutions extend the position-trajectory control method for a class of systems, which moved with a constant power and non-hyperbolic AC units.

With the original fuel saving technique, we presented selectable traction motor optimization.

The solutions allow to improving the functionality of mobile robots, significant minimizing fuel consumption without deterioration the quality characteristics, such as accuracy and speed.

References

[1] J. B. Heywood, “Internal Combustion Engine Fundamentals,” McGraw-Hill, 1988, 930 p.

[2] V. Kh. Pshikhopov, “Position-trajectory Control of Moving Objects,” TTI SFU, 2009, 183 p.

[3] V. Kh. Pshikhopov, M. Yu. Medvedev, R. V. Fedorenko, M. Yu. Sirotenko, V. A. Kostyukov, B. V. Gurenko, “Control of Aeronautic Complexes: Theory and Design Technology,” Fizmatlit, 2010, 394 p.

[4] A. T. Le, “Modelling and Control of Tracked Vehicles. Sydney,” University of Sydney, 1999, 208 p.

[5] J. Y. Wong, “Theory of Ground Vehicles,” Wiley, 2008, 592 p.

[6] D. B. Pogosov, “Synthesis and Analysis of Mathematical model of Highly-maneuverable Tracked Robots,” *Journal KBNC RAN 1*, pp. 301–306, 2011.

[7] L. V. Sergeev, “Tank Theory,” Academy publishing, 1973, 493 p.

[8] A. B. Vinogradov, “Vector Control of AC Motors,” Ivanovo, 2008, 297 p.

[9] V. V. Pankratov, “Vector Control of Induction Motors,” Novosibirsk, 1999, 66 p.

[10] A. A. Usoltzev, “Frequency Control of Induction Motors,” ITMO, 2006, 94 p.

[11] A. I. Voldek, “Electric Machienes,” Energiya, 1978, 832 p.

[12] V. I. Klyuchev, “Theory of Electric Drive,” Energoatomizdat, 1998, 697 p.

[13] M. G. Chilikin, A. S. Sandler, “General Course of Electric Drive,” Energoatomizdat, 1981, 576 p.

[14] A. Bennassar, A. Abbou, M. Akherraz, M. Barara, “Sensorless sliding mode control of induction motor using fuzzy logic Luenberger observer,” *Recent Advances in Neural Networks and Fuzzy System*, pp. 46–52, Mar. 2014.

[15] D. Pogosov, “Position-Trajectory Control of Advanced Tracked Robots with Diesel-Electric Powertrain,” *Robot Intelligence Technology and Applications 2*, vol. 274, pp. 393–403, Dec. 2013.

[16] J. Jung, K. Nam, “A vector control scheme for EV induction motors with a series iron loss model,” *IEEE Transactions on Industrial Electronics*, vol. 45, no. 4, pp. 617–624, Aug. 1998.

[17] G. Renukadevi, K. Rajambal, “Modeling and Analysis of Multi-Phase Inverter Fed Induction Motor Drive with Different Phase Numbers,” *WSEAS Transactions on Systems and Control*, issue 3, vol. 8, pp. 73–80, Jul. 2013.

[18] M. Jankovic, I. Kolmanovsky, “Constructive Lyapunov Control Designfor Turbocharged Diesel Engines,” *IEEE-transactions on Control Systems Technology*, vol. 8, no. 2, pp. 288–299.

[19] D. Yanakiev, I. Kanellakopoulos, “Engine and Transmission Modeling for Heavy-Duty Vehicles,” PATH, 1995, 64 p.

[20] J. H. Chang, B.-K. Kim, “Minimum-time minimum-loss speed control of induction motors under field-oriented control,” *IEEE Transactions on Industrial Electronics*, vol. 44, no. 6, pp. 809–815. 1997.

[21] A. B. Ali, R. Abdelati, M. F. Mimouni, R. Dhifaoui, “Maximum-Torque and Maximum-Efficiency Rotor Flux Selection of an Induction Motor in Transient Regime,” *International Journal of Sciences and Techniques of Automatic control & computer engineering*, vol. 4, no. 2, pp. 1370-1387. 2010.

[22] A. Kabanov, “Optimal Control of Mobile Robot’s Trajectory Movement,” *WSEAS Transactions on Systems and Control*, vol. 9, pp. 398–404. 2014.

[23] D. Pogosov, “Transformation of High-order Spline-functions to implicit form,” *SWorld conference proceedings 3*, vol. 4, pp. 84–87, Jun. 2012.